ELSEVIER

Physica B 301 (2001) 276–285

PHYSICA B

www.elsevier.com/locate/physb

Polarized Raman and infrared vibrational analysis of $(VO)_2P_2O_7$ single crystals

U. Kuhlmann[a,*], C. Thomsen[a], A.V. Prokofiev[b], F. Büllesfeld[b], E. Uhrig[b], W. Assmus[b]

[a] *Institut für Festkörperphysik, Technische Universität Berlin, Hardenbergstrasse 36, D-10623 Berlin, Germany*
[b] *Physikalisches Institut, Universität Frankfurt, D-60054 Frankfurt, Germany*

Received 20 October 2000

Abstract

Single crystals of the low dimensional spin system compound $(VO)_2P_2O_7$ were studied by polarized Raman spectroscopy and FT-IR spectroscopy in the spectral range 100–1400 cm^{-1}. Characteristic groups of modes were compared with literature data of structurally related compounds. Though some differences to vibrational spectra of the referred compounds were detected, we achieved a satisfactory assignment of most of the high-energy modes to vibrations of the P_2O_7 polyhedra and the VO_5 pyramids. In particular, we report the observation of an unusual softening of the prominent V=O vibration which we explain by the interlayer interaction of neighboring V and O atoms—an effect, which has been observed in NaV_2O_5, as well.

PACS: 63.20. − e; 63.20.Ry; 63.22. + m

Keywords: Raman spectroscopy; Infrared spectroscopy; Single crystals; $(VO)_2P_2O_7$

1. Introduction

Vanadyl pyrophosphate ($(VO)_2P_2O_7$) as a low dimensional spin system is subject to current interest because of the magnetic properties of its V^{4+} sublattice. Initially it has been proposed to possess model character for a two-legged Heisenberg spin ladder by, among others, Johnston et al. [1] and was investigated theoretically by Barnes and Riera [2]. Subsequent investigations revealed that the magnetic properties are dominated by alternating antiferromagnetic spin-$\frac{1}{2}$ chains along the crystallographic *b* direction [3,4].[1] Meanwhile, most observation support the model of two independent alternating antiferromagnetic spin-chains, which gives a plausible explanation for the second excitation first observed in inelastic neutron scattering experiments [3]. In Ref. [5] we report on the observation of the second spin-gap by Raman scattering and thus could resolve a discrepancy

* Corresponding author. Tel.: + 49-30-314-22476; fax: + 49-30-314-27705.
E-mail address: kuhli@physik.tu-berlin.de (U. Kuhlmann).

[1] Throughout this paper we denote the crystal axes in accordance with Ref. [8], i.e. the longest edge of the crystallographic unit cell is the *b* axis.

0921-4526/01/$ - see front matter
PII: S0921-4526(01)00238-1

between light-scattering experiments [6] on the one hand and neutron scattering, susceptibility and NMR experiments on the other hand.

A coupling of the spin system to the lattice vibrations was reported in Ref. [6] for three phonons in the low-energy region. Grove et al. observed an anharmonicity in the temperature dependence of the phonon frequency, which they attributed to the interaction of phonons with the spin system for phonon energies below the maximum of the magnon dispersion at ≈ 15.5 meV (125 cm^{-1}). The details of the spin–phonon coupling in $(VO)_2P_2O_7$ are, however, not yet cleared up. A full analysis of all phonons in the large unit cell, to our knowledge, has not been performed before.

Recently, single crystals of macroscopic size have become available [7], and we report polarized and depolarized Raman spectra as well as infrared phonon spectra from all three crystal surfaces. Based on a full group–theoretical analysis and on a comparison to known compounds with similar bonds we are able to assign the modes in the high-energy region (> 550 cm^{-1}) of the compound. The structure of $(VO)_2P_2O_7$ was first published by Gorbunova and Linde et al. [8]. The crystallographic unit cell comprises 8 formula units of $(VO)_2P_2O_7$. The compound consists of chains of VO_5 polyhedra, which are linked along the *b*-axis through the terminal bonds of $P_2O_7^{4-}$ double-polyhedra (Fig. 1). The $P_2O_7^{4-}$ connect these chains in [1 0 0] direction via their P–O–P bridging bonds to a three dimensional structure.

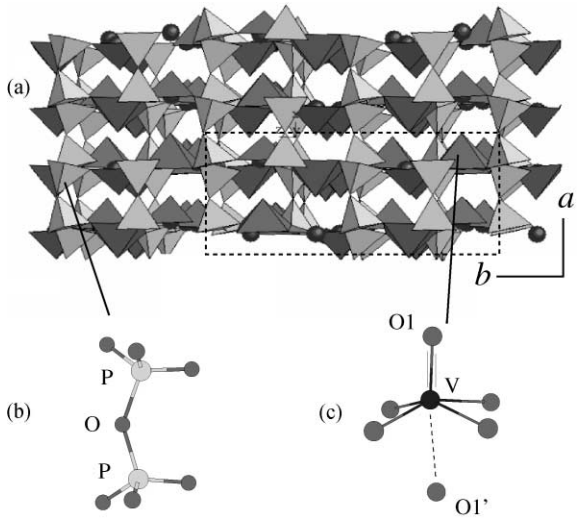

Fig. 1. (a) Structure of $(VO)_2P_2O_7$ crystal in $Pca2_1$ symmetry viewed along the *c*-axis. The dashed box represents the size of the unit cell in the *a*–*b* plane. The pyramidal environment of the vanadium atoms is depicted dark gray, the P_2O_7 polyhedra light gray. (b) The P_2O_7 group consist of two PO_3 tetraeder connected by an apical oxygen atom building the P–O–P bridge. (c) Shows the pyramidal vanadium environment in which the vanadium atom is double-bonded to the apical oxygen O1. Additionally it is weakly bonded to the neighboring oxygen O1′ which influences the strength of the V=O1 bond.

2. Experimental procedure

The $(VO)_2P_2O_7$ sample, a single crystal with a size of approximately 1 mm^3, was prepared as described by Prokofiev et al. [7]. Polarized Raman spectra were recorded with a DILOR XY 800 triple spectrometer in combination with a liquid nitrogen cooled CCD. The spectral resolution was 1.3 cm^{-1}, as exitation we used the 5683 Å line of an Kr^+ laser. The sample was mounted in a liquid helium bath cryostate and measurements were performed at 5 K and at room temperature. The room temperature IR-reflectivity spectra were recorded with a BRUKER IFS 66v fourier spectrometer, with the spectral resolution set to 2 cm^{-1}. The IR spectra were Kramers–Kronig transformed and the phonon frequencies determined from the maxima in the imaginary part of the transform.

3. Factor group analysis

The crystal structure of $(VO)_2P_2O_7$ has been examined experimentally in several studies, and the general conclusion is that it belongs to the orthorhombic system $Pca2_1$, with eight formula units per crystallographic unit cell [8,9]. A detailed refinement of X-ray data by Nguyen et al suggests a monoclinic $P2_1$ structure [10]. However, the differences between the structures are very small and presumably related to the crystal production process. An X-ray study on our samples which followed up the Raman measurements confirmed the orthorhombic $Pca2_1$ symmetry and thus justified the choice of

Table 1
Summary of the factor group analysis of $(VO)_2P_2O_7$. R, T, r and i.r. denotes rotations, translations, Raman active modes and IR active modes, respectively

Factor group species C_{2v}	8 P_2O_7 (C_1 sites)		16 VO (C_1 sites)		V C_1	P C_1	O C_1	Optical modes	Acoustic modes
	Internal modes	External modes	Internal modes	External modes					
A_1 (r, i.r.)	42	6T, 6R	4	12T, 8R	12	12	54	77	1
A_2 (r)	42	6T, 6R	4	12T, 8R	12	12	54	78	0
B_1 (r, i.r.)	42	6T, 6R	4	12T, 8R	12	12	54	77	1
B_2 (r, i.r.)	42	6T, 6R	4	12T, 8R	12	12	54	77	1
	168	24T, 24R	16	48T, 32R	48	48	216	309	3

Table 2
Correlation scheme for the internal modes of $P_2O_7^{4-}$ in $(VO)_2P_2O_7$

Free ion symmetry C_{2v}	Site symmetry C_1	Factor group symmetry C_{2v}
7 A_1	21 A	21 A_1 (r, i.r.)
4 A_2		21 A_2 (r)
4 B_1		21 B_1 (r, i.r.)
6 B_2		21 B_2 (r, i.r.)

this symmetry for our factor group analysis. To obtain an overview over the phonon spectra we assumed the pyrophosphate polyhedra to possess C_{2v} point symmetry as a close approximation to the true structure. In the refinement of Ref. [10] this polyhedra has C_1 point symmetry and would give us almost no information from the correlation scheme.

The factor group analysis was performed using the tables provided by Rousseau et al. [11] and is summarized in Table 1. The correlation scheme for the internal modes of the P_2O_7 groups is given in Table 2. Without the external modes $(VO)_2P_2O_7$ will possess $46A_1 + 46A_2 + 46B_1 + 46B_2$ Raman-active vibrations with selection rules $xx, yy, zz(A_1)$ and $xy(A_2)$, $xz(B_1)$, $yz(B_2)$ and $46A_1 + 46B_1 + 46B_2$ infrared-active vibrations with polarizations z, x, y, respectively. Most of the observed Raman lines were found to coincide with IR lines, confirming the assignment of the structure to the noncentrosymmetric 29th space group.

4. Results and discussion

We base the assignment of the observed spectral features to vibrations of the P_2O_7 and VO polyhedra on a comparison with structurally related materials. The phonon spectra of the pyrophosphate (diphosphate, P_2O_7) group was studied intensively in solution [12,13], in melted [14,15] and in crystalline compounds [16–21]. All authors accordingly found that the pyrophosphate vibrations are distributed with decreasing frequency in the order $\nu_{as}PO_3 > \nu_sPO_3 > \nu_sPOP > \delta OPO > \delta POP$, which was established by Bues et al. [14]. ν_{as} and ν_s refer to asymmetric and symmetric stretching vibrations of the terminal (PO_3) or bridge (POP) bonds, respectively; δ refers to the corresponding-bond bending vibrations, which are naturally lower in frequency. The frequencies for each of these types of vibrations in different compounds are always within the same frequency range, so that an unambiguous assignment of the high-energy modes of $(VO)_2P_2O_7$ is possible.

In comparison to the pyrophosphate group with 21 vibrational modes of the free molecule (symmetry C_{2v}) the diatomic vanadyl group exhibits only one stretching vibration, which in the crystal splits into four modes for all possible symmetries (see Table 1). Its frequency was found to depend on

bond length as well as on crystalline surrounding. The vanadium atoms are situated in a pyramidal environment of oxygen atoms (Fig. 1). Its base is formed by the terminal oxygen atoms of the P_2O_7 groups and with the oxygen atom O1 of the vanadyl group on top of the pyramid. The apical oxygen O1 is bonded to the vanadium ion with a relatively short bond length of 1.57 Å, whereas the base corner oxygens have distances to the vanadium atom of about 2 Å. The short bond is typical of the V=O vanadyl group which involves both π and σ bonding. This distorted pyramidal or octahedral environment, if we consider the apical oxygens (O1′) of neighboring layers, too, with one short V=O bond is characteristic for other vanadium phosphor oxides and vanadates like NaV_2O_5. We will compare studies on those materials with our results and discuss differences in structure and frequency.

The Raman spectra of $(VO)_2P_2O_7$, Fig. 2 displays an overview, revealed many lines which are concentrated in three energy regions. The most prominent peaks appear at 920 cm^{-1} (see inset of Fig. 2). These peaks become weak ($< 5\%$) in the depolarized geometries (xy, zx, yz), and we therefore assign them to A_1 symmetry. A second group of peaks is found in the high-energy region from 1050 to 1250 cm^{-1}, 3 of which are seen in A_1 scattering geometry and 13 in A_2, B_1 and B_2 geometries (Fig. 3). Below 500 cm^{-1} we found a multitude

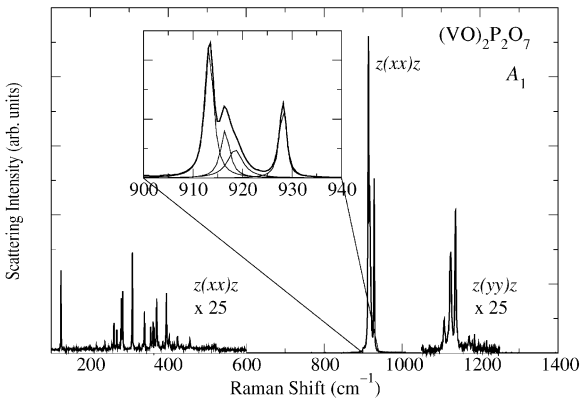

Fig. 2. Raman spectra of $(VO)_2P_2O_7$ at 5 K in A_1 symmetry. Shown in the inset is an expanded view and a four line least squares fit to the largest peaks around 915 cm^{-1}.

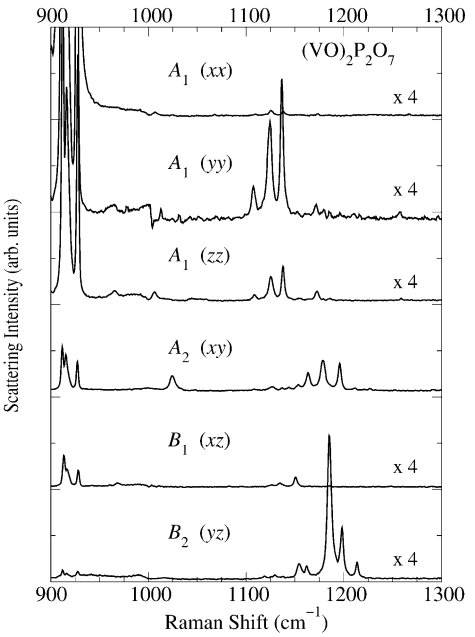

Fig. 3. High-energy part of the Raman spectra of $(VO)_2P_2O_7$ at 5 K. These modes are due to the PO_3 stretching vibrations in the P_2O_7 polyhedra.

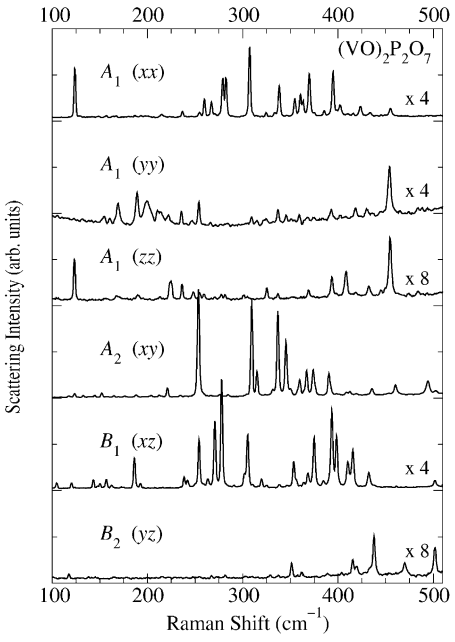

Fig. 4. Low-energy part of the Raman spectra of $(VO)_2P_2O_7$ at 5 K.

Table 3
Spectral data and band assignments of $(VO)_2P_2O_7$ of the modes above 700 cm^{-1}. The assignments to particular types of vibrations refer to groups of modes separated by horizontal lines except the γ_{as}POP vibration, which is assigned to the IR mode at 937 cm^{-1}

IR-reflectance			Raman shift						Assignment
x	*y*	*z*	*xx*	*yy*	*zz*	*xy*	*xz*	*yz*	
		743w							ν_sPOP
	750w		750vw	750vw	750vw				
			913vs	913vs	913vs				νVO
			917vs	917vs	917vs				
	919w		919vs	919vs	919vs				
926s			929vs	929vs	929vs				
937vs		939w							ν_{as}POP
		976vs		965w	965w				$\nu_s PO_3$
		1011s			1005w				
				1020w		1024m			
1062vs				1047vw	1047vw				
		1083w							
			1108w	1108s	1108s				
1113m									
		1120m							
			1125w	1125s	1125s	1127vw			$\nu_{as} PO_3$
1131vs							1135vw		
			1137w	1137s	1137s				
1147s		1146vs				1153w	1151vw		
								1155m	
								1162m	
		1165s				1164s			
	1172w			1170m	1170m	1178s			
		1188s						1185s	
						1196s			
								1198s	
		1200s							
		1216s						1214s	
	1219vs								
	1242vs								
	1262vs								

Intensity: vs very strong, s strong, m medium, w weak, vw very weak

of lines in all scattering geometries (Fig. 4). The observed modes above 700 cm^{-1} are summarized in Table 3. Besides these main features weak structures were found at 800 and 1000 cm^{-1}. We will first discuss the main Raman peaks at 920 cm^{-1} and then continue in descending order of frequency, beginning with the modes at 1200 cm^{-1}.

The polarized IR reflection spectra showed a similar subdivision as observed in the Raman spectra (Fig. 5). The most intense peaks are in the region between 900 and 1300 cm^{-1}, and several less intense peaks are observed below 650 cm^{-1}. Differences were found in the position of the main peaks in *x*, *y* and *z* polarizations, respectively. We performed a Kramers–Kronig transformation on these spectra to obtain the frequencies of the underlying phonon modes from the calculated absorbance and summarized the ones above 700 cm^{-1} in Table 3, as

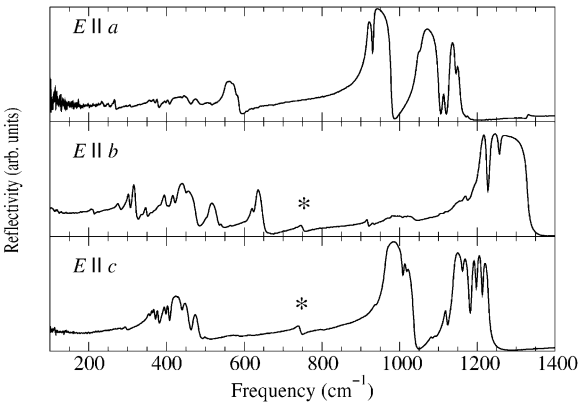

Fig. 5. Room temperature polarized far-infrared reflectivity spectra of $(VO)_2P_2O_7$ single crystals for the $E\|a$, $E\|b$ and $E\|c$ polarizations. The symmetric P–O–P bond stretching vibration appears in y and z polarization and is marked by an asterisk.

well. Summing up these calculated absorbances we obtained a spectrum which is comparable to an (unpolarized) transmission spectrum of $(VO)_2P_2O_7$ and found good correspondence to already published unpolarized IR data on $(VO)_2P_2O_7$ and related compounds [21,22]. Comparing our measurements at 5 K and room temperature we found no evidence for a structural phase transformation. The phonon anomaly of the modes near 123 cm^{-1} was confirmed although it was not quite as strong as in Ref. [6]. With the exception of the modes around 915 cm^{-1} which will be discussed below, all other vibrational modes generally harden by less than 1% when lowering the temperature from 293 to 5 K.

4.1. VO vibrations

The strong Raman peak around 915 cm^{-1} consists of four lines at 913, 917, 919 and 929 cm^{-1}, as can be seen in the expanded view in Fig. 2. All peaks are most intense in xx polarization and less but equally intense in yy and zz polarizations (Fig. 3). The number of lines and the polarization fit well with the assignment of this mode to the stretching vibrations of the vanadyl groups, which are oriented along the a crystal axis (Fig. 1). The splitting into four modes arises from the four slightly different crystal sites of the VO_5 pyramids in the large crystallographic unit cell. In crystalline V_2O_5 and alkali vanadates like LiV_2O_5 and NaV_2O_5 the related vibrations were found to exhibit frequencies at 994, 984 and 969 cm^{-1}, respectively [23–25]. Although the VO_5 pyramids are stacked in a similar way in the vanadates and in $(VO)_2P_2O_7$, the interlayer distance between the vanadium atom and the apical oxygen atom from neighboring layers (V–O1′) is smaller in $(VO)_2P_2O_7$. This distance was found to influence strongly the vanadyl vibrational frequency, which was demonstrated by Loa et al. by Raman scattering under pressure on NaV_2O_5 [26,27]. They found that the frequency of the V=O bond weakens from 969 to $\sim$ 919 cm^{-1} when applying a pressure of 15 GPa, in connection with a contraction of the c-axis and the decrease in the V–O1′ interlayer distance from 3 to 2.3 Å. The increasing influence of the interlayer V–O1′ bond effectively weakens the intralayer V=O1 bond which leads to the observed softening. In $(VO)_2P_2O_7$ at atmospheric pressure the distance is approximately 2.3 Å and the Raman frequencies match those in NaV_2O_5 under high pressure, thus confirming our assignment to the V = O stretching vibrations.

This picture is further supported by the observation of an up to now unreported anharmonicity of these modes as a function of temperature. Fig. 6 shows the relative frequency shift of two of the four modes between room temperature and 5 K. The two other ones which are not depicted show similar behavior. The modes exhibit a softening of 0.5% (about 5 cm^{-1}) upon cooling. Both the application of hydrostatic pressure on the crystal, as shown with NaV_2O_5, and the lowering of the temperature result in a contraction of the crystallographic unit cell. Hence through the decreasing layer distance the interlayer V–O1′ bond influences increasingly the intralayer V=O1 bond, which in effect lowers the V=O1 mode frequency. (The observed frequency shift of about 5 cm^{-1} corresponds to a specific shift of 0.017 cm^{-1}/K.) If we suppose this mechanism to work comparably in NaV_2O_5 and $(VO)_2P_2O_7$, a simple linear estimate would give a contraction of the crystallographic a-axis of 0.08 Å from room temperature to 5 K and thus give a linear thermal expansion coefficient of

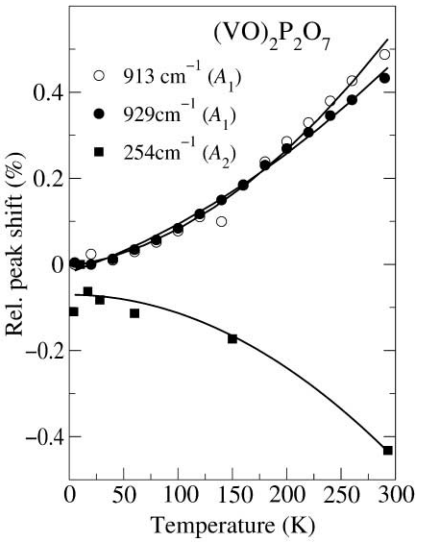

Fig. 6. Temperature-induced relative shifts of the vibrational frequencies of the A_1 Raman modes around 915 cm^{-1} with respect to the positions at 5 K (open and filled circles). The modes at 917 and 919 cm^{-1} (not shown) have the same shift. The modes exhibit a frequency softening of 0.5% upon cooling from room temperature to 5 K. In contrast to that most of the other vibrational modes show an upshift upon cooling. The mode at 254 cm^{-1} (squares) is depicted as an example of the general behavior.

$\alpha_a \approx 3 \times 10^{-5}$ K^{-1}. This value, which has the same size as for other layered compounds,[2] could be proven by temperature dependend X-ray scattering, which we have planned for the future. Similar compounds were studied in Refs. [28–30]. Mahadevan et al. [21] examined $Rb_3(VO)_3(P_2O_7)_2$ and $CsVOP_2O_7$. They observed the V=O stretching vibration at 978 cm^{-1} in the Cs compound and at 913 cm^{-1} in the Rb compound and related it to the different bond lengths of the apical oxygen of 1.592 and 1.606 Å, respectively. These numbers confirm both the plain dependence of the vibrational frequency on the V = O bond length and the influence of the crystal environment.

As the VO dipoles are almost entirely oriented along the *a*-axis of the $(VO)_2P_2O_7$ crystal, IR activity should occur in the corresponding polarization, which can be seen in Fig. 5, upper panel. Therefore we assigned the strong band at 926 cm^{-1} in the IR(x) spectra to the infrared active counterpart of the V = O vibration.

4.2. P_2O_7 vibrations

The asymmetric PO_3 terminal stretching vibrations ($\nu_{as}PO_3$) of the P_2O_7 group in different compounds are usually observed in the high-energy region from roughly 1050 to 1250 cm^{-1}. From the correlation of the free-ion symmetry to the factor group symmetry 32 asymmetric PO_3 stretching modes are expected in the Raman spectra, 8 in each of the symmetries A_1, A_2, B_1 and B_2, respectively, 24 of them being IR active as well. We observed 4 strong or medium intense modes in A_1, 3 in A_2 and 5 in B_2 symmetry, respectively. In the $y(**)y$ scattering geometry we observed only 2 weak modes in A_2 symmetry, which may be due to the generally weaker scattering efficiency on this surface.

The IR spectra revealed 12 medium or intense peaks between 1100 and 1300 cm^{-1}. With the exception of the modes with the highest energy ($\geqslant$ 1219 cm^{-1}), the majority of the observed vibrational frequencies are close to those of the Raman lines which supports the premise of the crystal structure not being centrosymmetrical. The number of observed Raman and IR modes is smaller than predicted by the factor group analysis, which will be discussed below.

The frequencies of the symmetric PO_3 terminal stretching vibrations are, in general, expected below the asymmetric ones in the region between 900 and 1100 cm^{-1}. The factor group analysis predicts 4 Raman-active modes in each of the symmetries A_1, A_2, B_1 and B_2 and 12 IR active modes. We observed them in the Raman spectra as weak peaks at 965, 1005, 1020, 41047 cm^{-1} in A_1 symmetry and as a medium intense peak in A_2 symmetry at 1024 cm^{-1}. Strong modes appear in the IR spectra at 937, 976, 1011, 1062 and 1083 cm^{-1}. Again, the number of observed Raman and IR modes is smaller than predicted by group theory. For obvious physical reasons (see for example Ref. [19]) it has been established that those vibrational modes of

[2] For example the interlayer thermal expansion coefficient in graphite $\alpha_c \approx 3 \times 10^{-5}$ K^{-1} [32].

the factor group are strong in the Raman spectra, which are derived from totally symmetric vibrational modes of the free-ion and, vice versa, those are strong in the IR spectra, which are derived from antisymmetric free-ion vibrations. If we consider the correlation of the terminal stretching modes of the P_2O_7 polyhedra to the factor group symmetry, we find in A_1 symmetry (with the symmetry of the free-ion mode given in parentheses) $2\nu_s(A_1)$ and $2\nu_{as}(A_1)$ modes and the same numbers for the other symmetries allowed in the factor group. Whereas this argument holds reasonably for the region of the $\nu_{as}PO_3$ vibrations, where 3 stronger peaks could be observed in most scattering geometries, it fails for the region of the ν_sPO_3 modes, where only weak peaks with less than $\frac{1}{3}$ of the intensity of the $\nu_{as}PO_3$ vibrations could be observed. This is one of the remarkable differences of the spectra of $(VO)_2P_2O_7$ in comparison to other compounds containing P_2O_7 groups. In the alkaline earth compounds α-$Ca_2P_2O_7$, α-$Sr_2P_2O_7$ and α-$Ba_2P_2O_7$ the ν_sPO_3 vibrations appear as dominant peaks between 1050 and 1100 cm^{-1} [17], whereas the $\nu_{as}PO_3$ have lower intensities in the spectra. A similar picture is given by the Raman spectra of $Rb_2(VO)_3(P_2O_7)_2$ [21] or $Fe_2P_2O_7$ [30]. Our observations concerning the intensities of the terminal stretching vibrations are supported by the unpolarized spectra of $(VO)_2P_2O_7$ reported in Ref. [22], which—much less resolved—show a similar distribution of spectral features as our measurements.

In the IR spectra strong modes appear between 900 and 1000 cm^{-1} in x and z polarization, which we assign to the ν_sPO_3 vibrations. Whereas this assignment is satisfactory for the z polarization, it is not free of ambiguity in the x polarization. Here we had expected the V=O vibrations assigned to the 926 cm^{-1} mode before as well as the asymmetric ν_{as}POP bridge stretching vibration. In y polarization we observed only weak reflection structures in the spectral region under discussion. A possible explanation could be the strong anisotropy of the crystal structure along the $b(y)$ and $c(z)$ axis. The first is the direction of the alternating V^{4+} chains and the anisotropy could result in different dipole moments for the ν_sPO_3 vibrations along the b and c axis.

The νPOP-bridge bending vibrations are to a certain extent characteristic for the P_2O_7 polyhedra, since in the free-ion symmetry C_{2v} there is only one symmetric ν_sPOP vibration (A_1) and one asymmetric ν_{as}POP vibration (B_2). Factor-group splitting leads to 2 symmetric or asymmetric bridge stretching vibrations in all representations of the group C_{2v}^5. On the above stated grounds that crystal modes derived from symmetric or antisymmetric molecular vibrations are strong in the Raman or IR spectra, respectively, the symmetric vibration is usually (i.e. in a variety of compounds) found to appear strongly in the Raman spectra around 750 cm^{-1} [17–20], whereas the IR activity depends on the amount of the P–O–P angle and disappears with vanishing dipole moment when the bridge is stretched linearly. The frequency of the ν_{as}POP vibration is expected to be about 200 cm^{-1} higher than the symmetric one.

We observed the symmetric POP stretching vibration in the IR spectra in y and z polarization at 750 and 743 cm^{-1}, respectively (Fig. 5). A closer examination of the polarization of the free-ion vibration as well as the orientation of the pyrophosphate groups on the two inequivalent sites within the crystal unit cell reveals that the set of P_2O_7 polyhedra with P–O–P angles of 161° is oriented to interact predominantly with radiation polarized in z direction whereas the set of P_2O_7 polyhedra with angles of 144° interacts predominantly with y polarized light. The conclusion would be that the different P–O–P angles result in different bond stretching vibrational frequencies, with the smaller bonding agles resulting in the higher frequency. This question has been addressed by Sarr et al. [31] by comparing different hydrogenopyrophosphates. They found no correlation of bond angles to ν_sPOP from one compound to another, but this does not necessarily hold for different bond angles within one compound. For the same reasons which have been mentioned in the discussion of the νPO_3 vibrations the ν_sPOP vibration, as derived from a totally symmetric free-ion mode, is expected to appear in the Raman spectra with fairly large intensity. Surprisingly this was not found to be the case and the mode appears only very weakly in the Raman spectra at 750 cm^{-1}. We assigned the asymmetric ν_{as}POP stretching vibration to

a strong peak in the IR spectra at 937 cm^{-1}. If this mode has the same frequency in the Raman spectra, it may be hidden by the very strong vanadyl vibrations around 920 cm^{-1}.

In the spectral region below 600 cm^{-1} the PO_3 terminal bending vibrations are expected. Since about two thirds of all internal modes of the P_2O_7 group appear in this region, an unambiguous assignment of vibrational modes to spectral features was not possible. In the study of Sarr et al. [31] a linear relation between the bridge angle and the frequency of the bridge bending vibration δPOP was established. Applying this relation to the vanadyl anion of $(VO)_2P_2O_7$ and considering bridge angles of 144 and 161°, we expect Raman and IR lines around 300 and 245 cm^{-1}, respectively. A specific assignment was not carried out although some candidates for this mode are present in both the Raman and the IR spectra. Below roughly 220 cm^{-1} external modes of the pyrophosphate and vanadyl units are observed. The low frequency modes at 70, 118 and 123 cm^{-1}, which have been reported to interact with the spin system [6], presumably originate from rigid vibrations of the VO_5 or P_2O_7 polyhedra.[3]

5. Summary and conclusions

Single crystals of $(VO)_2P_2O_7$ were examined by polarized Raman and infrared spectroscopy. We observed more than 80 phonon modes of which we assigned the high frequency ones (around 915 cm^{-1}) to the V=O stretching vibrations and, by comparison with other compounds, the highest frequency ones to vibrations of the P_2O_7 polyhedra. The assignment to V=O out-of-plane stretching vibrations is strongly supported by the observation of an unusual peak shift as a function of temperature of these modes. It is explained by the interaction of the V atom with oxygen atoms of neighboring layers from the similarity with the pressure effect observed in α-NaV_2O_5. By analogy with the data of Loa et al. [26] on pressure dependent Raman scattering on α-NaV_2O_5, we roughly estimate a thermal expansion coefficient of $(VO)_2P_2O_7$ along the crystallographic *a*-axis to $\alpha_a \approx 3\times10^{-5}\ K^{-1}$, a rather large value but typical for layered compounds. In contrast to these modes most of the other modes reveal a normal behavior as a function of temperature, i.e. they exhibit a slight mode hardening with decreasing temperature.

The low frequency modes are more or less evenly distributed between $\approx$ 100 and $\approx$ 600 cm^{-1}, originating from bond bending modes and external modes of the VO_5 and P_2O_7 polyhedra. To most of the observed Raman modes we found infrared counterparts, which is in accordance with the assignment of the noncentrosymmetric $Pca2_1$ space group to the crystal structure. Some vibrational modes, which are usually strong in related compounds, were found to be weak in $(VO)_2P_2O_7$.

[3] The anharmonic mode at 123 cm^{-1} we find in (*xx*) and (*zz*) scattering geometry different from Ref. [6] where it was reported to occur in all parallel polarizations.

Acknowledgements

Fruitful discussions with Z.V. Popović are gratefully acknowledged. This work was supported by Deutsche Forschungsgemeinschaft, through SPP 1073.

References

[1] D.C. Johnston, J.W. Johnston, D.P. Goshorn, A.J. Jacobson, Phys. Rev. B 35 (1987) 219.
[2] T. Barnes, J. Riera, Phys. Rev. B 50 (1994) 6817.
[3] A.W. Garrett, S.E. Nagler, D.A. Tennat, B.C. Sales, T. Barnes, Phys. Rev. Lett. 79 (1997) 745.
[4] J. Kikuchi, K. Motoya, T. Yamauchi, Y. Ueda, Phys. Rev. B 60 (1999) 6731.
[5] U. Kuhlmann, C. Thomsen, A. Prokofiev, F. Büllesfeld, E. Uhrig, W. Assmus, Phys. Rev. B 62 (2000) 12262.
[6] M. Grove, P. Lemmens, G. Güntherodt, B.C. Sales, F. Büllesfeld, W. Assmus, Phys. Rev. B 61 (2000) 6126.
[7] A.V. Prokofiev, F. Büllesfeld, W. Assmus, Crystal Res. Technol. 33 (1998) 157.
[8] Y.E. Gorbunova, S.A. Linde, Sov. Phys. Doklady 24 (1979) 138.
[9] Z. Hiroi, M. Azuma, Y. Fujishiro, T. Saito, M. Takano, F. Izumi, T. Kamiyama, T. Ikeda, J. Solid State Chem. 146 (1999) 369.

[10] P. Nguyen, R. Hoffman, A. Sleight, Mat. Res. Bull. 30 (1995) 1055.
[11] D. Rosseau, R. Bauman, S. Porto, J. Raman Spectrosc. 10 (1981) 253.
[12] E. Steger, C. Fischer-Bartelk, Z. Anorg. Allg. Chemie 338 (1965) 15.
[13] H. Eysel, K.T. Lim, J. Raman Spectrosc. 19 (1988) 535.
[14] W. Bues, H.-W. Gehrke, Z. Anorg. Allg. Chem. 288 (1956) 291.
[15] W. Bues, K. Bühler, P. Kuhnle, Z. Anorg. Allg. Chem. 325 (1963) 8.
[16] A. Hezel, S. Ross, Spectrochimica Acta 23A (1967) 1583.
[17] B. Cornilsen, R. Condrate, J. Solid State Chem. 23 (1978) 375.
[18] B. Cornilsen, R. Condrate, J. Inorg. Nucl. Chem. 41 (1979) 602.
[19] B. Cornilsen, J. Mol. Struct. 117 (1984) 1.
[20] N. Santha, V. Nayar, G. Keresztury, Spectrochim. Acta 49A (1993) 47.
[21] V.P. Mahadevan Pillai, B.R. Thomas, V. Nayar, K.-H. Lii, Spectrochim. Acta Part A 55 (1999) 1809.
[22] I. Kanesaka, K. Osaki, I. Matsuura, J. Raman Spectrosc. 26 (1995) 997.
[23] P. Clauws, J. Broeckx, J. Vennik, Phys. Stat. Sol. B 131 (1985) 459.
[24] X. Zhang, R. Frech, Electrochimica Acta 42 (1997) 475.
[25] Z.V. Popović, M.J. Konstantinović, R. Gajić, V. Popov, Y.S. Raptis, A.N. Vasil'ev, M. Isobe, Y. Ueda, Solid State Commun. 110 (1999) 381.
[26] I. Loa, U. Schwarz, M. Hanfland, R. Kremer, Phys. Stat. Sol. B 215 (1999) 709.
[27] I. Loa, K. Syassen, R. Kremer, Solid State Commun. 112 (1999) 681.
[28] C. Julien, I. Ivanov, A. Gorenstein, Mater. Sci. Eng. B33 (1995) 168.
[29] J. Gaubicher, Y. Chabre, J. Angenault, A. Lautié, M. Quarton, J. Alloys Compounds 262–263 (1997) 34.
[30] E. Baran, I. Botto, A. Nord, J. Mol. Struct. 143 (1986) 151.
[31] O. Sarr, L. Diop, Spectrochim. Acta 43A (1987) 999.
[32] B. Brockhouse, G. Shirane, in: M. Balkanski (Ed.), Lattice Dynamics, Flammarion Sciences, Paris, 1977, p. 122.